AD-A271 827

MENTATION PAGE

Form Approved
OMB No. 0704-0188

2. REPORT DATE	3. REPORT TYPE AND DATES COVERED
24 September 1993	REPRINT

4. TITLE AND SUBTITLE

Structure and Morphology of Pd Overlayers on Epitaxial SnO_2 Films Studied with the Atomic Force Microscope

5. FUNDING NUMBERS

61103d3484A7

6. AUTHOR(S)

R. J. Lad, M. J. Matthews, M. D. Antonik, R. E. Cavicchi, and S. Semancik

7. PERFORMING ORGANIZATION NAME(S) AND ADDRESS(ES)

Laboratory for Surface Science and Technology
5764 Sawyer Research Center
University of Maine
Orono, ME 04469-5764

AFOSR-TR- 93 0[illegible]3

8. PERFORMING ORGANIZATION REPORT NUMBER

9. SPONSORING/MONITORING AGENCY NAME(S) AND ADDRESS(ES)

AFOSR/NC
Building 410
Bolling AFB
Washington, DC 20332-6448

10. SPONSORING/MONITORING AGENCY REPORT NUMBER

AFOSR-90-0258

11. SUPPLEMENTARY NOTES

Mat. Res. Soc. Symp. Proc. Vol. 280 (1993) pp. 641-644

12a. DISTRIBUTION/AVAILABILITY STATEMENT

APPROVED FOR PUBLIC RELEASE; DISTRIBUTION UNLIMITED

12b. DISTRIBUTION CODE

13. ABSTRACT *(MAXIMUM 200 WORDS)*

The structure and morphology of clean and Pd-doped epitaxial SnO_2 films were studied with the atomic force microscope (AFM). The SnO_2 films were grown by reactive sputter deposition on three different substrates yielding epitaxial orientations: (101) SnO_2 / *r*-cut sapphire, (100) SnO_2 / basal sapphire, and (110) SnO_2 / TiO_2 (110). AFM imaging of monolayer amounts of Pd deposited onto the epitaxial SnO_2 films shows that the Pd is dispersed at 300 K and forms clusters after annealing to 500 K in vacuum.

14. SUBJECT TERMS

Atomic Force Microscopy, Gas Sensors, Pd-doped SnO_2 Films

15. NUMBER OF PAGES

4

16. PRICE CODE

17. SECURITY CLASSIFICATION OF REPORT	18. SECURITY CLASSIFICATION OF THIS PAGE	19. SECURITY CLASSIFICATION OF ABSTRACT	20. LIMITATION OF ABSTRACT
UNCLASSIFIED	UNCLASSIFIED	UNCLASSIFIED	SAME AS REPORT

Mat. Res. Soc. Symp. Proc. Vol 280 (1993) pp 641-644

STRUCTURE AND MORPHOLOGY OF PD OVERLAYERS ON EPITAXIAL SnO_2 FILMS STUDIED WITH THE ATOMIC FORCE MICROSCOPE

R.J. LAD*, M.J. MATTHEWS*, M.D. ANTONIK*, R.E. CAVICCHI ** AND S. SEMANCIK**
* Laboratory for Surface Science & Technology, 5764 Sawyer Research Center, University of Maine, Orono, ME 04469-5764
** Chemical Science and Technology Laboratory, National Institute of Standards and Technology, Gaithersburg, MD 20899

ABSTRACT

The structure and morphology of clean and Pd-doped epitaxial SnO_2 films were studied with the atomic force microscope (AFM). The SnO_2 films were grown by reactive sputter deposition on three different substrates yielding epitaxial orientations: (101) SnO_2 / r-cut sapphire, (100) SnO_2 / basal sapphire, and (110) SnO_2 / TiO_2 (110). AFM imaging of monolayer amounts of Pd deposited onto the epitaxial SnO_2 films shows that the Pd is dispersed at 300 K and forms clusters after annealing to 500 K in vacuum.

INTRODUCTION

SnO_2 films are widely used as the active elements of gas sensing devices. These devices operate by relating chemisorption events to changes in the electrical characteristics of the film. For example, conductivity-based SnO_2 films have been used to detect reducing gases such as CO, H_2O, H_2 and CH_4 [1]. The exact response of these devices is determined by the interplay between the chemical, structural and electronic properties of the SnO_2 film [2,3].

The addition of monolayer amounts of metal dopants onto the surface of the gas sensing films has been shown to dramatically enhance the film sensitivity and selectivity to a target gas. In the case of SnO_2, studies of this effect have included Pd [4-6], Pt [7], and Al [8] dopants. While the sensing mechanisms are directly related to changes in the chemical and electrical characteristics of the film caused by the metal additives, these characteristics are strongly dependent on the microstructure and topology of the film.

In this paper, we focus on only one aspect of SnO_2 based gas sensors, namely the surface microstructure of SnO_2 films. Using the atomic force microscope, we have followed the changes in morphology of Pd dopants on epitaxial SnO_2 films as a function of annealing treatments.

EXPERIMENTAL

The epitaxial SnO_2 films were fabricated by r.f. reactive sputter deposition using a pure Sn target and equal pressures of argon and oxygen. The growth rate was approximately 5 Å / min and the substrate temperature was 500 °C; other details of the growth process are described elsewhere [9]. The SnO_2 films were grown on three different substrates: Al_2O_3 ($10\bar{1}2$) or r-cut sapphire, Al_2O_3 (0001)

or basal sapphire, and TiO_2 (110). Each of these substrates was mechanically polished to an "epitaxial grade" finish, cleaned with an aqua regia etch (sapphire) or acetone / methanol rinse (TiO_2), and preannealed in vacuum prior to film growth. The Pd overlayers were deposited on the SnO_2 films from a thermal evaporation source and the Pd coverage was referenced to a quartz crystal oscillator.

Atomic force microscope (AFM) imaging was performed using a commercial microscope which uses an optical lever deflection system in air. The images reported here were obtained using standard microfabricated Si_3N_4 cantilevers and pyramidal tips and using a constant no-load feedback condition.

CHARACTERIZATION OF EPITAXIAL SnO_2 FILMS

Atomic force microscope images of the surface morphology of 400 Å thick SnO_2 films deposited on the three different substrates are shown in Fig. 1. X-ray diffraction results [9] indicate that the SnO_2 films grow epitaxially with the

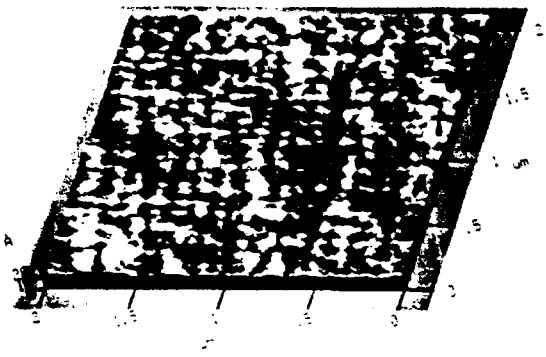

Fig. 1a SnO_2 (101) / Al_2O_3 ($10\bar{1}2$)
rms roughness = 1.2 Å
(2 μm x 2 μm area)

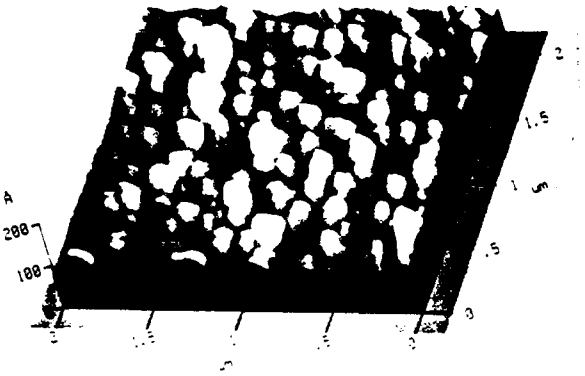

Fig. 1b SnO_2 (100) / Al_2O_3 (0001)
rms roughness = 12.3 Å
(2 μm x 2 μm area)

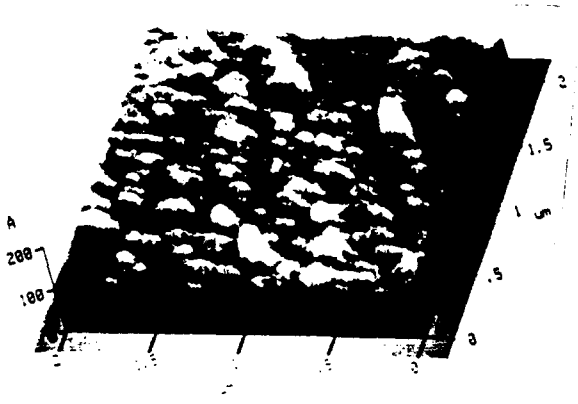

Fig. 1c SnO_2 (110) / TiO_2 (110)
rms roughness = 12.2 Å
(2 μm x 2 μm area)

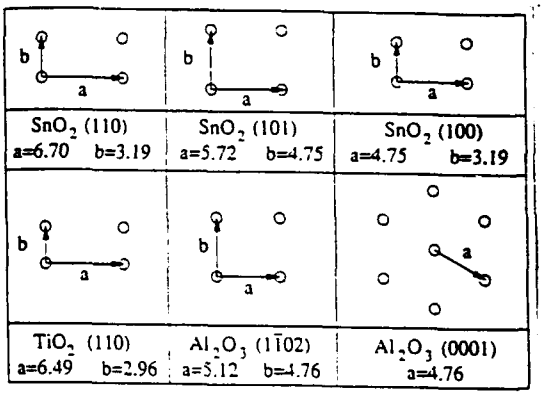

Fig. 1d Surface mesh dimensions of
the substrates and SnO_2 films

orientation the SnO_2 tetragonal (rutile) cell dictated by lattice matching with the substrate unit mesh as shown in Fig. 1d. The AFM results indicate that the film grown on the r-cut sapphire is superior to the films grown on basal sapphire and TiO_2 substrates both in terms of uniformity and surface roughness.

Atomic height steps were observed on the clean r-cut sapphire substrate with the AFM [10] and this step structure remains visible even after the growth of a 400 Å thick SnO_2 film as shown by striations aligned along the y-direction in Fig. 1a. These results indicate that the film grew via a layer-by-layer growth mechanism controlled by diffusion to step edges [11]. Films on the basal sapphire and TiO_2 substrates grow epitaxially but are an order of magnitude rougher than on the r-cut sapphire and contain grains approximately 150 nm in diameter.

MORPHOLOGY OF PD OVERLAYERS ON SnO_2 FILMS

AFM studies were carried out on the SnO_2 films following the deposition of 0.1, 1, 3 and 8 monolayers of Pd. The deposition procedure was the same for each sample and consisted of (i) annealing the SnO_2 film at 850 K for 3 min in UHV (ii) dosing 1 Torr of O_2 for 3 min at 700 K (iii) cooling to 300 K and then pumping away the O_2 and (iv) dosing Pd at 300 K at a rate of 0.25 monolayers / min. Samples were then immediately imaged by AFM or annealed at 500 K for 3 min in UHV without exposing the Pd to air prior to AFM imaging.

At the two lowest Pd coverages, AFM imaging revealed small changes in surface morphology, but it was difficult to conclusively differentiate Pd-derived features from the SnO_2 morphology, particularly on the rough SnO_2 / basal sapphire and SnO_2 / TiO_2 films. However, at the 3 monolayer and 8 monolayer Pd coverages, the Pd features are clearly visible.

Figure 2 shows AFM images obtained from a SnO_2 (101) / r-cut sapphire sample dosed with 8 monolayers of Pd. The morphology after Pd deposition at 300 K is shown in fig 2a. The step structure visible on the surface of the SnO_2 film

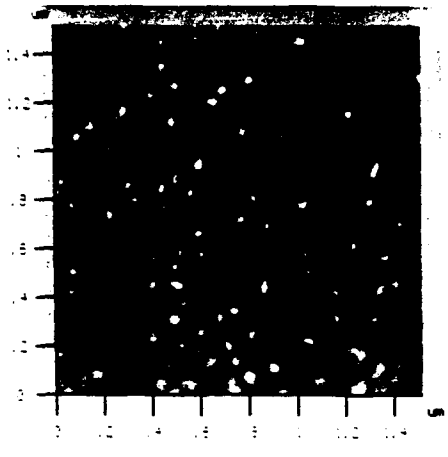

Fig. 2a
8 monolayers of Pd deposited on SnO_2 (101) / r-cut sapphire at 300 K
(1.5 μm x 1.5 μm; 25 Å gray-scale)

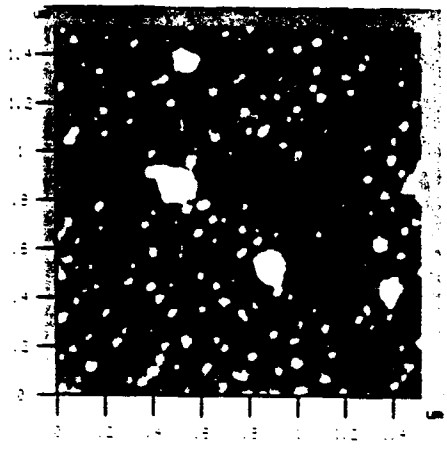

Fig. 2b
8 monolayers of Pd on SnO_2 / r-cut sapphire annealed at 500 K for 3 min
(1.5 μm x 1.5 μm; 25 Å gray-scale)

is retained and is decorated by dispersed islands of Pd which are approximately 30 nm in diameter. An identical sample was prepared, except it was annealed at 500K for 3 min in UHV following the Pd deposition. The resulting AFM image (fig. 2b) shows larger clusters of Pd which are approximately 50 nm in diameter. These images show direct evidence for ripening of the dispersed Pd islands into larger clusters with the annealing treatment. This result also agrees with previous XPS and conductivity measurements for the Pd / SnO_2 system [4].

One limitation of the AFM is that the long range tip-surface force interactions can lead to image artifacts that are due to the finite size and shape of the tip. This effect is important when the size of the features being imaged are comparable to the radius of curvature of the tip. In this study, the shape and lateral size of the Pd clusters is uncertain because of this limitation. However, the vertical resolution is reliable to within 1 Å. We also observed that image artifacts could be produced by scribing the Pd overlayers with the AFM tip at large repulsive loads.

CONCLUSIONS

The atomic force microscope was used to characterize the surface morphology of prototypical SnO_2 and Pd / SnO_2 gas sensing films. Layer-by-layer epitaxial growth of monocrystalline SnO_2 (101) films was achieved on r-cut sapphire substrates. Pd overlayers deposited onto the SnO_2 films at 300 K exhibit a dispersed morphology that evolves into clusters upon annealing to 500 K.

ACKNOWLEDGMENTS

This work was partially funded by the Air Force Office of Scientific Research. MJM gratefully acknowledges support from the McNair Scholars Program.

REFERENCES

[1] J. Janata, Anal. Chem. **64**, 196R (1992) and references therein.
[2] G. Heiland, Sensors and Actuators **2**, 343 (1982).
[3] W. Göpel, Prog. Surf. Sci. **20**, 9 (1985).
[4] T. Fryberger, J.W. Erikson and S. Semancik, Surf. Interface Anal. **14**, 83 (1989).
[5] T. Fryberger and S. Semancik, Sensors and Actuators **B2**, 305 (1990).
[6] J. Klöber, M. Ludwig and H.A. Schneider, Sensors and Actuators **B3**, 69 (1991).
[7] L. De Angelis and N. Minnaja, Sensors and Actuators **B3**, 197 (1991).
[8] C. Xu, J. Tamaki, N. Miura and N. Yamazoe, Sensors and Actuators **B3**, 147 (1991).
[9] S. Semancik and R.E. Cavicchi, Thin Solid Films **206**, 81 (1991).
[10] M.D. Antonik and R.J. Lad, J. Vac. Sci. Technol. **A10**, 669 (1992).
[11] R.E. Cavicchi, S. Semancik, M.D. Antonik and R.J. Lad, Appl. Phys. Lett. **61**, 1921 (1992).